

STOPPING COOLING FLOWS WITH COSMIC RAY FEEDBACK

WILLIAM G. MATHEWS¹
Draft version October 24, 2018

ABSTRACT

Multi-Gyr two-dimensional calculations describe the gasdynamical evolution of hot gas in the Virgo cluster resulting from intermittent cavities formed with cosmic rays. Without cosmic rays, the gas evolves into a cooling flow, depositing about 85 solar masses per year of cold gas in the cluster core – such uninhibited cooling conflicts with X-ray spectra and many other observations. When cosmic rays are produced or deposited 10 kpc from the cluster center in bursts of about 10^{59} ergs lasting 20 Myrs and spaced at intervals of 200 Myrs, the central cooling rate is greatly reduced to $\dot{M} \approx 0.1 - 1$ solar masses per year, consistent with observations. After cosmic rays diffuse through the cavity walls, the ambient gas density is reduced and is buoyantly transported 30-70 kpc out into the cluster. Cosmic rays do not directly heat the gas and the modest shock heating around young cavities is offset by global cooling as the cluster gas expands. After several Gyrs the hot gas density and temperature profiles remain similar to those observed, provided the time-averaged cosmic ray luminosity is about $L_{cr} = 2.7 \times 10^{43}$ erg s⁻¹, approximately equal to the bolometric cooling rate L_X within only ~ 56 kpc. If an appreciable fraction of the relativistic cosmic rays are protons, gamma rays produced by pion decay following inelastic p-p collisions may be detected with the Fermi Gamma Ray Telescope.

Subject headings: X-rays: galaxies: clusters — galaxies: clusters: general — cooling flows — cosmic rays — gamma rays: theory

1. INTRODUCTION

X-ray spectra of hot virialized gas in galaxy groups and clusters have firmly established that the rate that gas cools to low temperatures is much lower than that expected from uninhibited radiative cooling in subsonically inflowing cooling flows (e.g. Peterson et al. 2001). As a result of this realization, many theoretical and computational studies have sought to prevent cooling inflows by introducing a gas heating mechanism usually exploiting the phenomenal accretion energy released by massive black holes in the cores of group and cluster-centered elliptical galaxies (e.g. McNamara & Nulsen 2007). In spite of this almost unlimited source of accretion energy, no specific mechanism or mode of gas heating has been accepted that is successful for long cosmic times and for cooling flows of all scales: galactic, group and cluster.

In their recent review of the cooling flow puzzle McNamara & Nulsen (2007) (MN07) emphasize two types of AGN-related heating mechanisms: PdV work done when cavities in the hot gas are inflated by cosmic rays (CRs) and energy-dissipating shock (or other) waves that deliver energy from the central energy source throughout the cluster gas. CRs, often observed inside cluster cavities from radio synchrotron emission, are thought to be deposited or produced by non-thermal jets that project out from the central AGN. However, our recent study of the energetics of cluster cavities inflated by CRs (Mathews & Brighenti 2008b = MB08) shows that the (shock) heating produced as young cavities expand due to locally enhanced CRs is more than compensated by a global cooling as the entire cluster gas expands more or less permanently to accommodate the partial pressure of the CRs as they diffuse into the cluster gas. Most of the

PdV work expended as cavities form is stored in potential energy of displaced gas that moves out in the cluster potential. The dissipative heating beneath buoyant cavities discussed in MN07 appears to be absent in the cavities computed in MB08, and this is consistent with our earlier estimate (Mathews et al. 2006). The total (bulk and turbulent) kinetic energy is always very small and cannot be an important source of dissipative heating (MB08).

The second currently favored heating mechanism, large scale wave dissipation, is also problematic. Since the hot gas density profiles in groups and clusters is generally flatter than $\rho \propto r^{-2}$, successive shocks preferentially heat gas near the cluster center until it exceeds observed temperatures (Mathews, Faltenbacher & Brighenti 2006). Over-heating the central gas is a persistent difficulty with previous theoretical attempts to resolve the cooling flow problem by using central AGN heating scenarios (Brighenti & Mathews 2002b, 2003) since the cluster gas closest to the source of AGN energy typically has the lowest temperatures observed in the hot cluster gas. Finely-tuned heating scenarios in which the gas inflow is assumed to be essentially stopped are inconsistent with secular changes in the gas that evolve without limit. For example metal enrichment by Type Ia supernovae in the central galaxy would eventually increase the local hot gas metal abundances far above those observed.

As an alternative solution to the cooling flow problem, we proposed that gas receiving AGN energy is buoyantly transported outward. In these mass-circulating flows gas flows in both radial directions simultaneously. The combined flows maintain a cooling flow appearance similar to observed X-ray images (Mathews et al. 2003, 2004; Brighenti & Mathews 2006).

In this Letter we describe the evolution of virialized hot gas in the Virgo cluster in which successive cavities

¹UCO/Lick Observatory, Dept. of Astronomy and Astrophysics, University of California, Santa Cruz, CA 95064

are formed with CRs that buoyantly transfer gas from near the cluster core to large radii where its radiative cooling time is very much longer. The average net gas mass that flows past every cluster radius is very small although significant inflows and outflows occur locally in the gas. In buoyant outflows generated by CRs, the cluster gas need not be directly heated by the CRs, although some modest heating results from the dissipation of weak shocks that propagate away from newly formed cavities (Mathews & Brighenti 2007; MB08). Unlike most AGN heating scenarios, buoyant mass-circulating flows generated by CRs can preserve the observed cluster temperature and density profiles for at least several Gyrs. This resolution of the cooling flow problem, using mass transfer by CR buoyancy rather than heating, is attractive because almost all group and cluster-centered galaxies are observed to produce CRs in jets, radio lobes, or in central non-thermal radio sources.

2. EQUATIONS AND PROCEDURE

The procedure and assumptions employed here are nearly identical to those described in detail by MB08 to which the reader is referred. The flow equations are

$$\frac{\partial \rho}{\partial t} + \nabla \cdot \rho \mathbf{u} = 0 \quad (1)$$

$$\rho \left(\frac{\partial \mathbf{u}}{\partial t} + (\mathbf{u} \cdot \nabla) \mathbf{u} \right) = -\nabla(P + P_c) - \rho \mathbf{g} \quad (2)$$

$$\frac{\partial e}{\partial t} + \nabla \cdot \mathbf{u} e = -P(\nabla \cdot \mathbf{u}) - (\rho/m_p)^2 \Lambda(T, z) \quad (3)$$

$$\frac{\partial e_c}{\partial t} + \nabla \cdot \mathbf{u} e_c = -P_c(\nabla \cdot \mathbf{u}) + \nabla \cdot (\kappa \nabla e_c) + \dot{S}_c \quad (4)$$

where artificial viscosity terms are suppressed. Gas and CR pressures are related to their corresponding energy densities by $P = (\gamma - 1)e$ and $P_c = (\gamma_c - 1)e_c$ respectively where for simplicity we assume $\gamma = 5/3$ and $\gamma_c = 4/3$ for fully relativistic CRs. The energy spectrum of the CR particles $N(E)$ is not considered in detail so the CRs are characterized only by their integrated energy density $e_c \propto \int EN(E)dE$. Furthermore, the CR particles are unspecified and can consist of electrons or protons in any combination.

Unlike the discussion in MB08, we now include radiative cooling. We adopt the radiative cooling coefficient $n_{ions} n_e \Lambda_{sd}(T, z)$ erg cm⁻³ s⁻¹ from Sutherland and Dopita (1993) which, as expressed in equation 3, $(\rho/m_p)^2 \Lambda$ erg cm⁻³ s⁻¹, requires that $\Lambda = 1.1[(4 - 3\mu)(2 + \mu)/25\mu^2] \Lambda_{sd}$ where $\mu = 0.61$ is the molecular weight and the coefficient is $n_{ions}/n_p = 1.1$. We do not compute the metallicity in the gas throughout the flow but simply adopt a uniform metallicity near solar $z = 0.75z_\odot$ since most of the gas that cools has been metal-enriched in the cluster core. The computed flows are not sensitive to the gas metallicity. Computational timesteps are required to be less than the constant-pressure radiative cooling time in all zones. Since some cooling occurs in off-center zones near the z -axis, it is useful to remove cooled gas from the computational grid. If a grid zone cools below $T_{min} = 5 \times 10^5$ K, gas is removed at constant pressure by reducing the zone density until the temperature resets to $T_{max} = 5 \times 10^6$ K. Gas removal

at constant pressure from a zone preserves the pressure gradients relative to nearby zones so the gas flow to or from neighboring zones is unaffected. Moreover, the total thermal energy in the zone is also preserved so thoroughly cooled gas removed in this way does not alter the total thermal energy of uncooled gas. We assume that CRs are not removed with the cooled gas.

Gas is accelerated by pressure gradients in both the thermal gas and CRs. The two fluids are assumed to be coupled by the presence of small magnetic fields in the cluster gas. This coupling can be efficient even when the energy density in the magnetic field is much less than that in the thermal gas, which is consistent with the small fields observed in clusters, 1 – 10 μ G (Govoni & Feretti 2004). Consequently, magnetic pressure and stresses are not explicitly considered.

Equation 4 above describes the advection of CRs by locally flowing gas and the diffusion of CRs through this gas. Little is known about the diffusion coefficient κ , but it is likely that it varies inversely with the gas density since the magnetic field is probably larger in denser gas. As in MB08 we consider a range of CR diffusion coefficients that depend on a single density parameter n_{e0} :

$$\kappa = \begin{cases} 10^{30} \text{ cm}^2 \text{ s}^{-1} & : n_e \leq n_{e0} \text{ cm}^{-3} \\ 10^{30} (n_{e0}/n_e) \text{ cm}^2 \text{ s}^{-1} & : n_e > n_{e0} \text{ cm}^{-3} \end{cases}$$

Here we consider $n_{e0} = 6 \times 10^{-3}$ and 6×10^{-6} cm⁻³. The cluster gas dynamics are not very sensitive to n_{e0} or to other $\kappa(n_e)$ variations that have been explored (MB08).

The flow equations are solved in 2D cylindrical coordinates (R, z) using a ZEUS-like code (Stone & Norman 1992) but with the additional CR equation. As in MB08 the computational grid consists of 100 equally-spaced zones out to 50 kpc plus an additional 100 zones in both coordinates that increase logarithmically out to ~ 1 Mpc, filling a large hemisphere. Also following MB08, a spherical gravitational potential for the Virgo cluster is found by assuming that the gas is in hydrostatic equilibrium with the temperature and modified density profiles $T_G(r)$ and $\rho_{mG}(r)$ observed by Ghizzardi et al. (2004). The density profile was found by integrating the equation of hydrostatic equilibrium using $T_G(r)$ and the total gravitational acceleration from a $3.2 \times 10^9 M_\odot$ black hole, the M87 stellar mass $\rho_*(r)$ from Brighenti & Mathews (2002a), and an NFW profile with $M_{vir} = 1.30 \times 10^{14} M_\odot$ and concentration 8.60. The resulting modified observed density profile $\rho_{mG}(r)$ agrees very well with that of Ghizzardi et al. $\rho_G(r)$ for $r \gtrsim 1$ kpc but avoids an unphysical maximum in $g(r)$ near ~ 4 kpc if $g(r)$ is found from $T_G(r)$ and $\rho_G(r)$. All flow calculations begin with $T_G(r)$ and $\rho_{mG}(r)$.

CRs are introduced at intervals of $t_{cyc} = 2 \times 10^8$ yrs in bursts lasting $t_{cav} = 2 \times 10^7$ yrs. These timescales are roughly consistent with the lifetimes of visible X-ray cavities and radio synchrotron electrons. If the CR luminosity during injection times is \dot{E}_c , the time-averaged CR luminosity is

$$\langle L_{cr} \rangle = 2(t_{cav}/t_{cyc}) \dot{E}_c, \quad (5)$$

assuming that CRs are injected into both cluster hemispheres by symmetric double jets. For comparison with

the cavity calculations in MB08, all cavities are assumed to form in a source region 10 kpc along the z -axis described by a normalized Gaussian profile. The CR source term in equation 4 is therefore

$$\dot{S}_c = \dot{E}_c \tau(t) \frac{e^{-((\mathbf{r}-\mathbf{r}_{cav})/r_s)^2}}{\pi^{3/2} r_s^3} \quad \text{erg cm}^{-3} \text{s}^{-1} \quad (6)$$

where \mathbf{r} is the distance from the origin, $r_s = 2$ kpc and $\tau(t)$ is unity during injection times and zero otherwise. All calculations described here continue for 3 Gyrs. For each assumed $\kappa(n_{e0})$ we vary \dot{E}_c , seeking that value for which the gas temperature and density profiles continue to agree best with profiles observed in Virgo. Except for radiative cooling and a variable \dot{E}_c , the parameters chosen here are identical to those discussed for single cavities by MB08.

3. RESULTS

The left column of Figure 1 illustrates the evolution of Virgo cluster gas as a pure radiatively cooling flow without CRs. The long-dashed lines show the radial gas density, temperature and pressure profiles after evolving for 3 Gyrs from the observed profiles. The evolved profiles are determined by ordering ρ , T and P in each computational zone by increasing distance from the origin $r = (R^2 + z^2)^{1/2}$, then averaging in appropriate bins Δr . After 3 Gyrs, $\rho(r)$ and $T(r)$ have evolved away from the initial (observed) profiles (solid lines). The ratio of gas entropy to its initial value (subscript 0), $\log(S/S_0) = \log(T/T_0) - (2/3)\log(\rho/\rho_0)$, decreases monotonically toward the cluster center where the gas cools in the central 1.5 kpc. The discrepancy in integrated mass of (uncooled) gas between the initial and evolved density profiles in the uppermost panel, $\Delta M = M(r, 3 \text{ Gyr}) - M(r, 0)$, peaks at $\sim 15 \text{ kpc}^3$. Between 2 and 3 Gyrs the quasi-steady cooling rate in the core is $\langle \dot{M} \rangle = 86 M_\odot \text{ yr}^{-1}$ for the entire Virgo cluster (both hemispheres)⁴.

Panels in the central column of Figure 1 show the corresponding evolution with CRs having a low CR diffusion coefficient κ with $n_{e0} = 6 \times 10^{-6} \text{ cm}^{-3}$. In this solution after 3 Gyrs the gas density and temperature remain close to the initial, observed profiles. The entropy in $25 \lesssim r \lesssim 100 \text{ kpc}$ is lowered by the accumulated buoyant arrival of gas from the cluster core (cf. MB08) that lost entropy by radiation. The modest entropy maximum near 10 kpc is probably due to heating by successive weak cavity shocks at this radius. The total mass of hot gas in each spherical annulus changes very little during the evolution, as expected from the small central mass cooling rate between 2 and 3 Gyrs, $\langle \dot{M} \rangle = 0.13 M_\odot \text{ yr}^{-1}$ (for both hemispheres). The cooling inflow has been almost completely balanced by the outward circulation of gas from the cluster core to large radii driven by CR buoyancy. The bottom panel shows that the CR pressure P_c after 3 Gyrs is about an order of magnitude less than the gas pressure within 100 kpc, but P_c/P decreases sharply

³ This suggests the approximate site to initiate buoyant outflow.

⁴ The mass cooling rate, found from the total mass of cooled gas removed during this time interval, is insensitive to T_{min} and T_{max} . For example, $\langle \dot{M} \rangle = 85 M_\odot \text{ yr}^{-1}$ with $T_{min} = 3 \times 10^5 \text{ K}$ and $T_{max} = 10^6 \text{ K}$.

beyond 100 kpc. In this solution the total (spherical) time-averaged CR luminosity is $\langle L_{cr} \rangle = 2.70 \times 10^{43} \text{ erg s}^{-1}$. The total CR energy delivered to each cavity is about $E_{cav} = 8.2 \times 10^{58} \text{ ergs}$.

The right column of panels in Figure 1 shows the identical evolution but with a much larger CR diffusion coefficient ($n_{e0} = 6 \times 10^{-3} \text{ cm}^{-3}$). As before, the gas density and temperature profiles remain essentially unchanged after 3 Gyrs with a total time-averaged CR luminosity $\langle L_{cr} \rangle = 2.60 \times 10^{43} \text{ erg s}^{-1}$. The total gas cooling rate between 2 and 3 Gyrs, $\langle \dot{M} \rangle = 1.15 M_\odot \text{ yr}^{-1}$, is only ~ 0.01 of the cooling flow rate without CRs.

4. DISCUSSION AND CONCLUSIONS

CR buoyancy efficiently arrests cooling inflows without requiring *ad hoc* heating or infusions of hot, non-relativistic gas in the cavities. In the two solutions with CRs gas cools at the center and along the z -axis out to about 3 - 5 kpc where the free fall time to the center is $\lesssim 10^7 \text{ yrs}$. If all this cooled gas were accreted by the central black hole, the efficiency required for accretion energy to produce enough CRs to maintain the observed gas profiles is $\eta_{cr} = \langle L_{cr} \rangle / \langle \dot{M} \rangle c^2$. We find $\eta_{cr} = 3.6 \times 10^{-3}$ and 3.9×10^{-4} respectively for the low and high κ solutions. But η_{cr} is probably underestimated since some of the cooled, dusty gas in group-centered elliptical galaxies is heated and buoyantly relocated far out into the hot gas (Temi, Brighenti, & Mathews 2007). The total CR luminosity required to (nearly) stop the Virgo cooling flow, $\langle L_{cr} \rangle = 2.60 \times 10^{43} \text{ erg s}^{-1}$, is equal to the (computed) bolometric X-ray luminosity within only $\sim 56 \text{ kpc}$.

The Fermi Gamma Ray Telescope may confirm that cooling inflows in Virgo and other nearby clusters are stopped with CR buoyancy. Gamma rays are created by neutral pion decays following inelastic p-p interactions between CRs and the thermal plasma. The integrated gamma ray flux ($\text{cm}^{-2} \text{ s}^{-1}$) above energy $E_{\gamma, min}$ is

$$F_\gamma(E_\gamma > E_{\gamma, min}) = \frac{1}{4\pi d^2} \int_{Virgo} dV \int_{E_{\gamma, min}}^{\infty} dE_\gamma q_\gamma(E_\gamma, r) \quad (7)$$

where $d = 16 \text{ Mpc}$ is the distance to Virgo and the specific photon emissivity, $q_\gamma(E_\gamma, r) \text{ cm}^{-3} \text{ s}^{-1} \text{ GeV}^{-1}$, is described by Pfrommer & Ensslin (2004) and Ando & Nagai (2008). Assume for simplicity that all CRs are relativistic protons having a power law momentum distribution $f(p_p, r) \propto p_p^{-\alpha}$ with $\alpha = 2.3$. Then after 3 Gyrs the integrated gamma ray photon flux from Virgo above $E_{\gamma, min} = 2 \text{ Gev}$ is $F_\gamma = 2 \times 10^{-9}$ or $3 \times 10^{-9} \text{ cm}^{-2} \text{ s}^{-1}$ respectively for the low and high κ solutions in Figure 1. These fluxes are near the detection threshold of the Fermi telescope, $\sim 10^{-9} \text{ cm}^{-2} \text{ s}^{-1}$ estimated by Ando & Nagai (2008) for extended sources. If half of the CRs are electrons, evidence of the AGN CRs that we require in Virgo may still be marginally visible with the Fermi Telescope. Additional CRs in Virgo may have been produced in shocks and turbulence accompanying mergers or in the accretion shock when baryons first fell into the Virgo potential (Loeb & Waxman 2000), but these are not considered here.

For both low and high κ solutions in Figure 1 the CR partial pressure $P_c/(P + P_c)$ increases toward the cluster center. This may seem surprising because all CRs are

injected at 10 kpc and diffusion into the dense, central gas is slow because κ decreases. This feature can be understood from the reaction of X-ray cavities on the cluster gas. As a young cavity buoyantly moves away from the cluster center, relatively cooler nearby gas concentrates underneath the cavity, then flows rapidly outward through the cavity along the z -axis (MB08). These jets or filaments of denser thermal gas move out beyond 10 kpc then later fall back under gravity into the cluster core (e.g. Mathews & Brighenti 2008a). It is likely that the central concentration of CRs occurs because they are advected in with each infalling filament, then become trapped by the relatively small κ in the dense central gas. CRs are a likely source of non-thermal pressure that is occasionally observed in the cores of hot galactic and cluster gas.

Figure 2 shows that the distribution of CRs in in Virgo after 3 Gyrs is concentrated in the core and along the z -axis. In a recent study of warm and cold gaseous filaments in the Perseus Cluster, Ferland et al. (2008a,b) find that the observed spectrum can be understood if some of the the emission lines are excited by collisions with CRs. The enhanced CR distribution in Figure 2 along the z -axis provides a natural source of CRs just where the cool radial filaments form. Although we do not compute the passively evolving magnetic field, it is expected to be stronger in denser thermal filaments and longitudinally oriented along the cool filaments due to the radial expansion of the filament flow along the z -axis.

The 2D cylindrical nature of our solution requires that all cavities and CR activity occur along the z -axis. The

relatively small number of double-double radio sources (Schoenmakers et al. 2000) indicates that successive CR jets can move along the same direction, as assumed here. Remarkably, the X-ray thermal filament in Virgo (Forman et al. 2007) that formed by a cavity $\sim 10^8$ years ago (Mathews & Brighenti 2008a) and its associated radio lobe lie in a different direction than the younger non-thermal jet in the central galaxy M87. Another indication that CR energy flows out in many different directions is the azimuthal variation of successive generations of X-ray cavities in Perseus and other clusters.

It is expected that the mass outflow due to CR buoyancy in Figure 1 also transports iron produced by Type Ia supernova inside the central galaxy into a quasi-spherical region 50-100 kpc in radius as observed in many groups and clusters (De Grandi et al. 2004). The outflows described here can also carry short-lived dust out to 5-10 kpc into the hot gas where its far-infrared emission is observed in many nearby galaxy groups (Temi, Brighenti, & Mathews 2007). Radial entropy variations qualitatively similar to those in Figure 1 have been observed in galaxy groups (Gastaldello et al. 2007; Sun et al. 2008). Finally, the outward mass transport can create an inflection in the density slope as in Figure 1, resembling the double-structured character of many density profiles observed.

Studies of the evolution of hot cluster gas at UC Santa Cruz are supported by NASA and NSF grants for which we are very grateful.

REFERENCES

- Ando, S. & Nagai, D. 2008, MNRAS 385, 2243
 Brighenti, F. & Mathews, W. G. 2006, ApJ, 643, 120
 Brighenti, F. & Mathews, W. G. 2003, ApJ, 587, 580
 Brighenti, F. & Mathews, W. G. 2002b, ApJ, 573, 542
 Brighenti, F. & Mathews, W. G. 2002a, ApJ, 567, 130
 De Grandi, S., Ettori, S., Monghetti, M. & Molendi, S. 2004, A&A, 419, 7
 Ferland, G. J., Fabian, A. C., Hatch, N. A., Johnstone, R. M., Porter, R. L., van Hoof, P. A. M., & Williams, R. J. R. 2008b, MNRAS (submitted) (arXiv0810.5372)
 Ferland, G. J., Fabian, A. C., Hatch, N. A., Johnstone, R. M., Porter, R. L., van Hoof, P. A. M., & Williams, R. J. R. 2008a, MNRAS, 386, 72L
 Forman, W. et al. 2007, ApJ, 665, 1057
 Ghizzardi, S., Molendi, S., Pizzolato, F. & De Grandi, S. 2004, ApJ, 609, 638
 Gastaldello, F. et al. 2007, ApJ, 669, 158
 Govoni, F. & Ferretti, L. 2004, International Journal of Modern Physics D, 13, 1549
 Mathews, W. G., Faltenbacher, A., & Brighenti, F. 2006, ApJ, 638, 659
 Mathews, W. G. & Brighenti, F. 2008b, ApJ, 685, 128 (MB08)
 Mathews, W. G. & Brighenti, F. 2008a, ApJ, 676, 880
 Mathews, W. G. & Brighenti, F. 2007a, ApJ, 660, 1137
 Mathews, W. G., Faltenbacher, A. & Brighenti, F. 2006, ApJ, 638, 659
 Mathews, W. G., Brighenti, F. & Buote, D. A. 2004, ApJ, 615, 662
 Mathews, W. G. et al. 2003, ApJ, 596, 159
 McNamara, B. R. & Nulsen, P. E. J. 2007, Annual Review Astronomy & Astrophysics, 18, 117 (MN07)
 Peterson, J. R., Paerels, F. B. S., Kaastra, J. S., Arnaud, M., Reiprich, T. H., Fabian, A. C., Mushotzky, R. F., Jernigan, J. G. & Sakelliou, I. 2001, A&A 365, L104
 Pfrommer, C. & Ensslin, T. A. 2004, A&A, 413, 17
 Schoenmakers, A. P., et al. 2000, MNRAS 315, 371
 Stone, J. M. & Norman, M. L. 1992, ApJS, 80, 753
 Sun, M. et al. 2008, ApJ (submitted) (arXiv0805.2320)
 Temi, P., Brighenti, F. & Mathews, W. G. 2007, ApJ, 666, 222

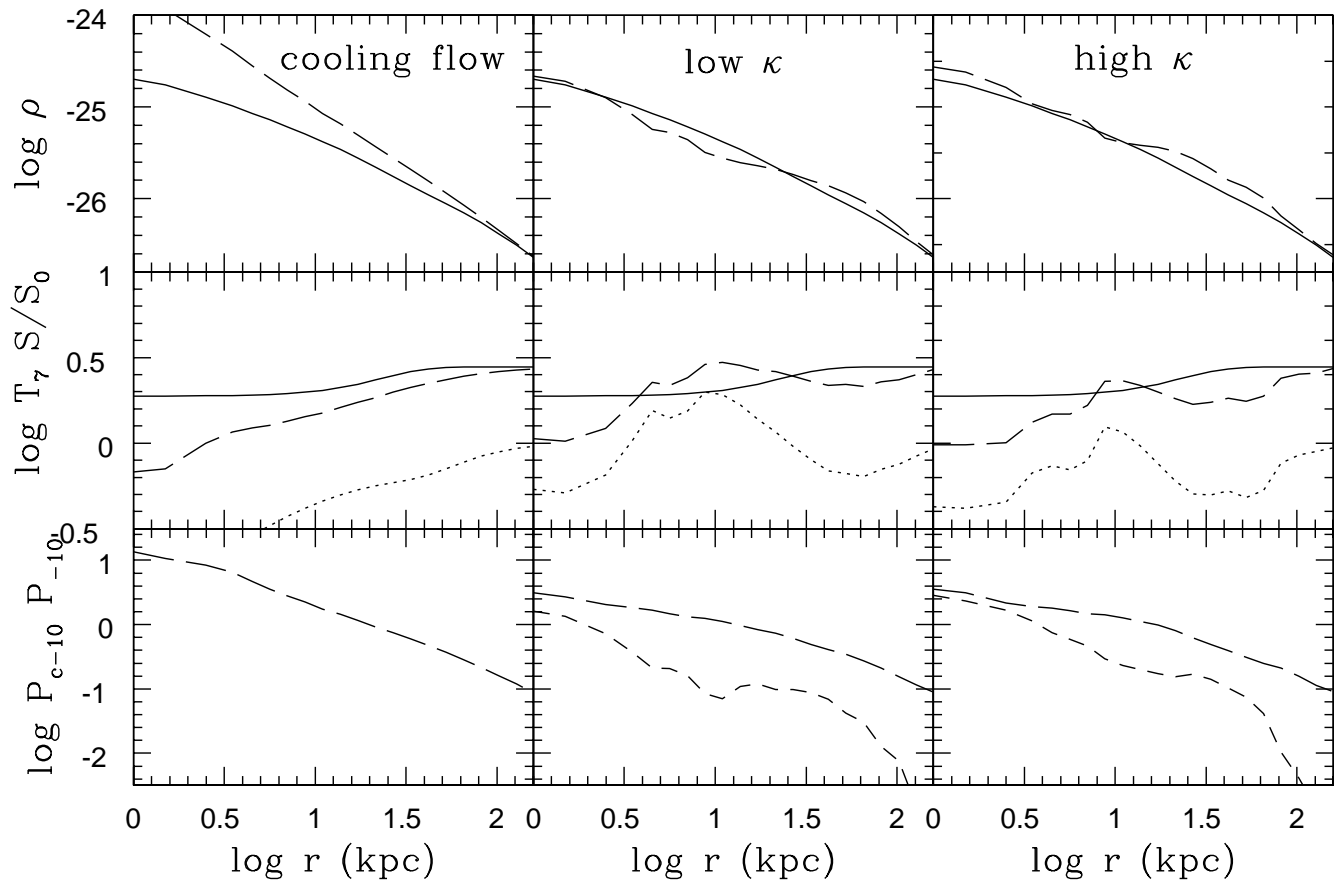


FIG. 1.— Radial distribution of gas and CRs in Virgo after 3 Gyrs of intermittent CR injection. Columns from left to right show a cooling flow without CRs, the same flow with weakly then strongly diffusing CRs. *Top row:* initial (observed) gas density (*solid lines*) and density after 3 Gyrs (*long dashed lines*). *Central row:* initial (observed) gas temperature (*solid lines*), and after 3 Gyrs (*long dashed lines*) (in units of 10^7 K) and the change $\log S/S_0$ of the gas entropy after 3 Gyrs (*dotted lines*). *Bottom row:* pressure of gas (*long dashed lines*) and CRs (*short dashed lines*) after 3 Gyrs (units of 10^{-10} dynes cm^{-2}).

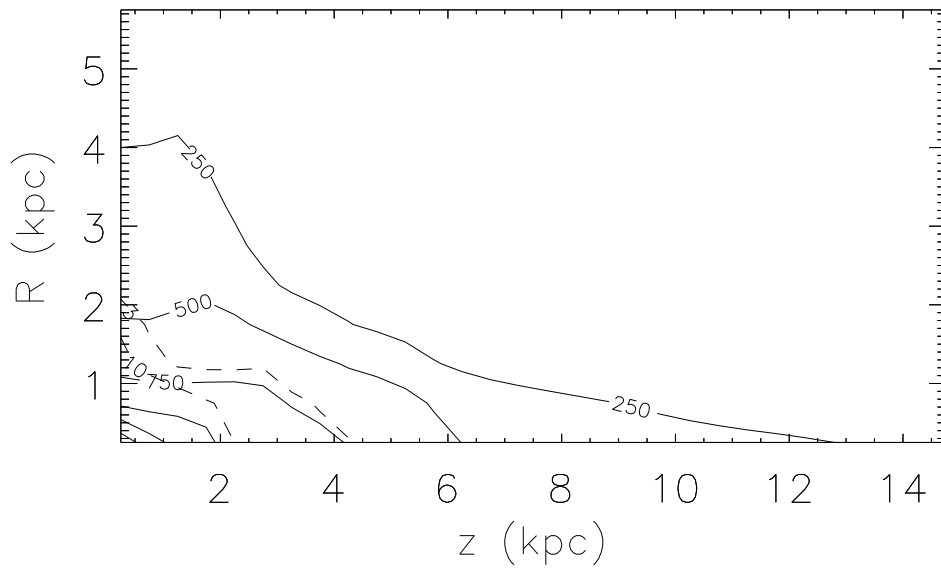


FIG. 2.— Distributions after 3 Gyrs of CR energy density $e_c(R, z)$ in units of 10^{-12} erg cm^{-3} (*solid lines*) and cooled mass in $10^8 M_\odot$ (*dashed lines*).